

H'_0 . The first and third terms in Eq. (D9) add up to the first term of Eq. (D8) to change the factor $\frac{3}{4}(1-\langle n_q \rangle)$, typical to the spin- $\frac{1}{2}$ problem, to a factor of $(\frac{1}{2}-\langle n_q \rangle)$, just like in the direct treatment of the Anderson model [cf. Eq. (3.1)], except for the difference in the effective J . The second term of Eq. (D9) together with Eq. (D10) produce the self-energy term

$$\sum_k [|V_k|^2 / (\epsilon_d - \epsilon_k)] (1 + \langle n_k \rangle),$$

which apart from the replacement of ω by ϵ_d is the same self-energy we encountered in Eq. (2.31).

Continuing now to the equations of motion for τ_{qd}^0 , we get in the same way

$$\begin{aligned} \langle \langle [\tau_{qd}^0, H_{\text{ex}}]; \xi_{ij}^\dagger \rangle \rangle &= -\frac{1}{4} \sum_k J_{qk} (1 - \langle n_q \rangle) \langle \langle \tau_{kd}^0; \xi_{ij}^\dagger \rangle \rangle \\ &\quad - \frac{3}{4} \sum_{k'/k} J_{k'k} \langle m_{k'q} \rangle \langle \langle \sigma_{ka}; \xi_{ij}^\dagger \rangle \rangle \\ &\quad + \frac{1}{2} \sum_{k'/k} J_{k'k} \langle m_{k'k} \rangle \langle \langle \sigma_{qd}; \xi_{ij}^\dagger \rangle \rangle, \end{aligned} \quad (\text{D11})$$

$$\begin{aligned} \langle \langle [\tau_{qd}^0, H_{\text{dir}}]; \xi_{ij}^\dagger \rangle \rangle &= \frac{1}{4} \sum_k J_{qk} (1 - \langle n_q \rangle) \langle \langle \tau_{kd}^0; \xi_{ij}^\dagger \rangle \rangle \\ &\quad + \frac{1}{2} \sum_k J_{kk} \langle n_k \rangle \langle \langle \tau_{qd}^0; \xi_{ij}^\dagger \rangle \rangle \\ &\quad - \frac{1}{4} \sum_{k'/k} J_{k'k} \langle m_{k'q} \rangle \langle \langle \sigma_{ka}; \xi_{ij}^\dagger \rangle \rangle + \sum_k W_{qk} \langle \langle \tau_{kd}^0; \xi_{ij}^\dagger \rangle \rangle, \end{aligned} \quad (\text{D12})$$

$$\langle \langle [\tau_{qd}^0, H'_0]; \xi_{ij}^\dagger \rangle \rangle = - \sum_k W_{kk} \langle \langle \tau_{qd}^0; \xi_{ij}^\dagger \rangle \rangle. \quad (\text{D13})$$

The first terms in Eqs. (D11) and (D12) cancel out and again the second term in Eq. (D12) together with (D13) produce the self-energy. From Eqs. (D8)–(D10) we get

$$\begin{aligned} \langle \langle \sigma_{qd}; \xi_{ij}^\dagger \rangle \rangle &= (\omega - \epsilon_q - \epsilon_d - \Sigma)^{-1} \{ \sum_k J_{kq} (\frac{1}{2} - \langle n_q \rangle) \langle \langle \sigma_{ka}; \xi_{ij}^\dagger \rangle \rangle \\ &\quad + \bar{\Sigma}_m \langle \langle \tau_{qd}^0; \xi_{ij}^\dagger \rangle \rangle + [\langle \sigma_{qd}; \xi_{ij}^\dagger \rangle] \} \end{aligned} \quad (\text{D14})$$

and from Eqs. (D11), (D12) and (D13) we get

$$\begin{aligned} \langle \langle \tau_{qd}^0; \xi_{ij}^\dagger \rangle \rangle &= (\omega - \epsilon_q - \epsilon_d - \Sigma)^{-1} \{ \bar{\Sigma}_m \langle \langle \sigma_{qd}; \xi_{ij}^\dagger \rangle \rangle \\ &\quad + [\langle \tau_{qd}^0; \xi_{ij}^\dagger \rangle] \}, \end{aligned} \quad (\text{D15})$$

where terms which are not logarithmically large or do not contribute to the special pole were dropped.

$\bar{\Sigma}_m$ is the equivalent of Σ_m of Sec. 4 and is given by

$$\bar{\Sigma}_m = \frac{1}{2} \sum_{k/k'} J_{k'k} \langle m_{k'k} \rangle. \quad (\text{D16})$$

It is clear that if we assume $\langle m_{k'k} \rangle$ to be diagonal in the Wannier representation and to be independent on the momenta, then $\bar{\Sigma}_m = 0$.

Field Effect on the Cochran Modes in SrTiO₃ and KTaO₃

E. F. STEIGMEIER

Laboratories RCA, Limited, Zurich, Switzerland

(Received 6 November 1967)

In connection with the Cochran theory of ferroelectricity, the thermal conductivity has been investigated in SrTiO₃ between 5 and 300°K and in KTaO₃ between 2.5 and 300°K. For temperatures above its maximum value, the conductivity shows an anomaly in SrTiO₃ which is absent in KTaO₃. This behavior is explained in terms of the degeneracy between the transverse optic (Cochran modes) and the longitudinal acoustic phonon branches. Measurements were also taken in electric fields up to 55 kV/cm, applied perpendicular to the temperature gradient. A considerable increase in thermal conductivity is observed in SrTiO₃ below 50°K, while the effect is much smaller in KTaO₃. An interpretation of this effect is given by assuming the transverse optic mode at $q=0$ to shift in frequency upon application of an electric field. An analysis of the experimental data in terms of a simple model is presented which leads to quantitative values for the frequency shifts in SrTiO₃. The results obtained for KTaO₃ indicate the presence of a phase transition of the non-ferroelectric type at 4.5°K, in analogy to the 103°K transition known for SrTiO₃.

INTRODUCTION

PEROVSKITES have attracted wide interest in the recent past since a theory of ferroelectricity in terms of lattice dynamics was developed.^{1,2} The strong temperature dependence of the transverse optic mode (Cochran mode), which was proposed, has since been fully established by measurements of infrared re-

flectivity³⁻⁶ and of inelastic neutron scattering.^{7,8} Cowley⁸ has found in SrTiO₃ that an accidental degeneracy between the transverse optic (TO) and the longitudinal acoustic (LA) mode occurs at \underline{q} around

³ A. S. Barker and M. Tinkham, Phys. Rev. **125**, 1527 (1962).

⁴ W. G. Spitzer, R. G. Miller, D. A. Kleinman, and L. E. Howarth, Phys. Rev. **126**, 1710 (1962).

⁵ A. S. Barker, Phys. Rev. **145**, 391 (1966).

⁶ R. C. Miller and W. G. Spitzer, Phys. Rev. **129**, 94 (1963).

⁷ R. A. Cowley, Phys. Rev. Letters **9**, 159 (1962).

⁸ R. A. Cowley, Phys. Rev. **134**, A981 (1964).

¹ P. W. Anderson, in *Fizika Dielektrikov*, edited by G. I. Skanavi (Acad. Nauk SSSR, Moscow, 1960), p. 290.

² W. Cochran, Advan. Phys. **9**, 387 (1960).

110°K for a considerable region in wave-vector space, and the degeneracy gradually extends to lower wave vectors (close to $q=0$) in lowering the temperature. The additional phonon interaction implied by this degeneracy should manifest itself in properties sensitive to phonon scattering, e.g., in thermal conductivity or in ultrasonic attenuation. The purpose of this work is to investigate this effect in thermal conductivity. SrTiO₃ and KTaO₃ were chosen for this study because these materials, although behaving lattice-dynamically in much the same way as other perovskites, exhibit no ferroelectricity since the TO mode frequency stays finite down to liquid helium temperatures.⁹⁻¹¹ Any complications caused by the ferroelectric state, such as, e.g., phonon scattering by ferroelectric domain walls, should therefore be absent.

An interesting problem is also the effect of a dc electric field on the Cochran mode.¹² The strong field dependence of the static dielectric constant^{13,14} at low temperatures suggests an analogous change in the TO mode frequency because of the connection between these two quantities.¹⁵ Thus, the phonon scattering might change upon application of an electric field. Preliminary measurements of Sievers¹⁶ seemed indeed to indicate such an effect. The present work is intended to study these phenomena in greater detail with the aim of deducing some value for the TO mode frequency shift with electric field.¹⁷

EXPERIMENTAL

The SrTiO₃ single crystals were obtained from National Lead Company. They are highly resistive ($\rho > 10^9 \Omega \text{ cm}$). A typical spectrographic analysis shows the following impurities: SiO₂, 20 ppm; Fe₂O₃, 10 ppm; Al₂O₃, 1 ppm; Sb₂O₃ < 1 ppm; W < 200 ppm; SnO₂, Mg, Cu, Pb, Mn, V, Cr, all < 0.1 ppm. The crystals were annealed at 1400°C for 24 h.

The KTaO₃ single crystals were grown at RCA Laboratories. Crystals 1 and 4 were clear and transparent, and crystal 55 was translucent. All of them exhibit a high resistivity ($\rho > 10^{11} \Omega \text{ cm}$). A typical spectrographic analysis shows for crystal 1 the following impurities: Fe, Cu < 10 ppm; Ba, Ca < 30 ppm; Al, Mg < 60 ppm; Li < 100 ppm; Na, Nb < 300 ppm.

⁹ P. A. Fleury and J. M. Worlock, *Phys. Rev. Letters* **18**, 665 (1967).

¹⁰ J. M. Worlock and P. A. Fleury, *Phys. Rev. Letters* **19**, 1176 (1967).

¹¹ G. Shirane, R. Nathans, and V. J. Minkiewicz, *Phys. Rev.* **157**, 396 (1967).

¹² E. Fatuzzo, *Proc. Phys. Soc. (London)* **84**, 709 (1964).

¹³ E. Sawaguchi, A. Kikuchi, and Y. Kadera, *J. Phys. Soc. Japan* **17**, 666 (1962); *Phys. Status Solidi* **6**, 333 (1964).

¹⁴ D. Itschner and H. Gränicher, *Helv. Phys. Acta* **37**, 624 (1964); D. Itschner, PhD thesis, Swiss Federal Institute of Technology, Zurich, 1965 (unpublished).

¹⁵ R. H. Lyddane, R. G. Sachs, and E. Teller, *Phys. Rev.* **59**, 673 (1941).

¹⁶ A. J. Sievers, *Bull. Am. Phys. Soc.* **8**, 208 (1963); and in *Proceedings of the Conference on Thermal Conductivity*, San Francisco, 1964 (unpublished).

¹⁷ A preliminary account of this work was given by E. F. Steigmeier and R. Klein, *Helv. Phys. Acta* **39**, 594 (1966).

The samples were oriented and cut to about 1×2×8 mm, all faces being {100}-oriented. Some measurements were taken also on samples of 2×4×8 mm. Thin gold or indium contacts were evaporated on the two opposite large-area faces for applying electric fields. A conventional steady-state longitudinal-heat-flow method was used to determine the thermal conductivity between 2 and 300°K. The apparatus is very similar to the one described by Slack.¹⁸ The temperature gradients along the sample (about 0.1 to 1.0°K per cm) were determined by means of gold+2.1 at.% cobalt-versus-manganin thermocouples. They were replaced later by gold+0.02 at.% iron-versus chromel thermocouples because the latter offer more sensitivity and stability at low temperatures. The thermocouples were glued with GE 7031 calorimeter cement onto the sample covered by a layer of cigarette paper as an electrical insulation. The thermocouple voltages were measured by means of a Keithley 148 nanovoltmeter. The heat input was determined electrically. The absolute temperature of the sample was determined below 14°K by means of a germanium thermometer, and above by means of a gas thermometer (content 100 cm³). To reduce the dead volume, Slack placed a membrane between the gas thermometer bulb and the pressure gauge (a precision ten-turn barometer was used in our case as a pressure gauge). This membrane, constructed as a double capacitor, was inserted into a capacitance bridge to serve as a null indicator. The voltage across the capacitance bridge at the same time served to drive a temperature controller. By using helium, nitrogen, and dry ice plus alcohol as cryogenic liquids, it was possible to reach any temperature in the range of 2 to 300°K and to stabilize the temperature to within 0.005°K in the helium range and to within 0.01°K above.

RESULTS

SrTiO₃

Figure 1 shows the results obtained for the thermal conductivity κ of SrTiO₃. A second sample of different dimensions gives the same curve for zero field. The results given in Fig. 1 agree very closely with the previous results for zero field by Sievers.¹⁶ They also agree with the more recent data of Suemune¹⁹ above 20°K. But there is a striking disagreement of them with very recent results of Hegenbarth²⁰ exhibiting some fine structure between 30 and 120°K. The reason for this is not clear.

The effect of an applied dc electric field of 23 kV/cm along the [100] direction and perpendicular to the heat flow is also shown in Fig. 1. It should be pointed out that these measurements are extremely delicate because of the contradictory requirements of good

¹⁸ G. A. Slack, *Phys. Rev.* **122**, 1451 (1961).

¹⁹ Y. Suemune, *J. Phys. Soc. Japan* **20**, 174 (1965).

²⁰ E. Hegenbarth, in *Proceedings of the International Meeting on Ferroelectricity, Prague, 1966*, edited by V. Dvorak, A. Fónskova, and P. Glogar (Institute of Physics of the Czechoslovak Academy of Science, Prague, 1966), Vol. I, p. 104.

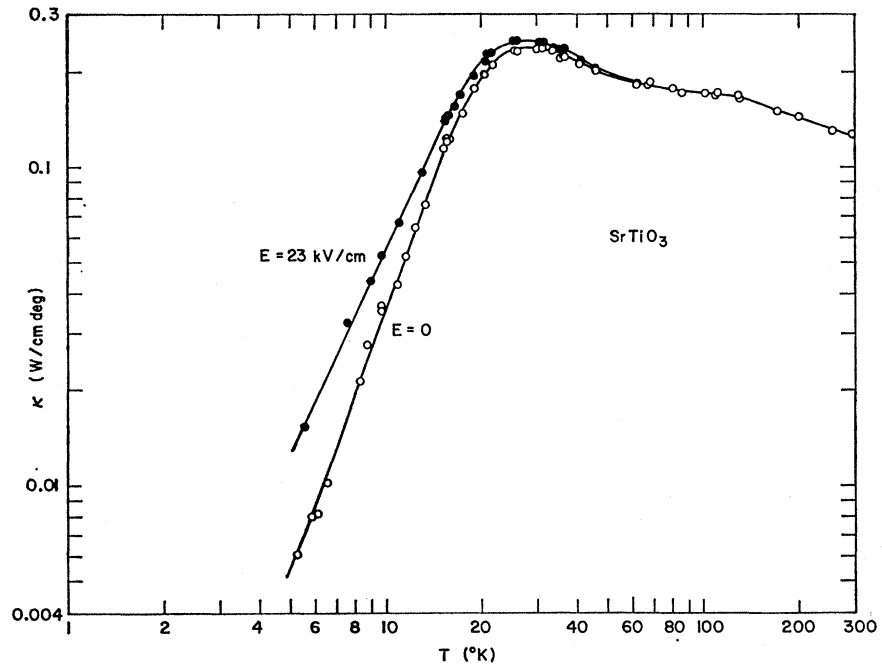


FIG. 1. The thermal conductivity of SrTiO₃ as a function of temperature without (○) and with (●) an electric field of 23 kV/cm applied to it.

thermal contact between sample and thermocouples and of good electrical insulation between field electrodes and thermocouples. A plot of the change in thermal conductivity due to the electric field ($\Delta\kappa = \kappa_E - \kappa$) is given in Fig. 2 as a function of temperature with electric field as a parameter. The curve exhibits a pronounced peak at 15°K. The previous data of Sievers¹⁶ showed a much smaller peak at 8°K and zero effect at 16°K. This discrepancy is not understood. In the present work, the maximum relative thermal conductivity change

$\Delta\kappa/\kappa$ is found at the lowest temperatures because of the rapidly decreasing κ . At 5°K, it amounts to about 1.5 for 23 kV/cm or 2 for 46 kV/cm. At 15°K, the temperature of the peak in Fig. 2, measurements were also taken as a function of the electric field up to 46 kV/cm. The results are shown in Fig. 3.

It might be mentioned here that a sample of 2-mm thickness (instead of 1 mm) produced the same field effect provided it was cooled in an electric field through the 103°K cubic-to-tetragonal phase transi-

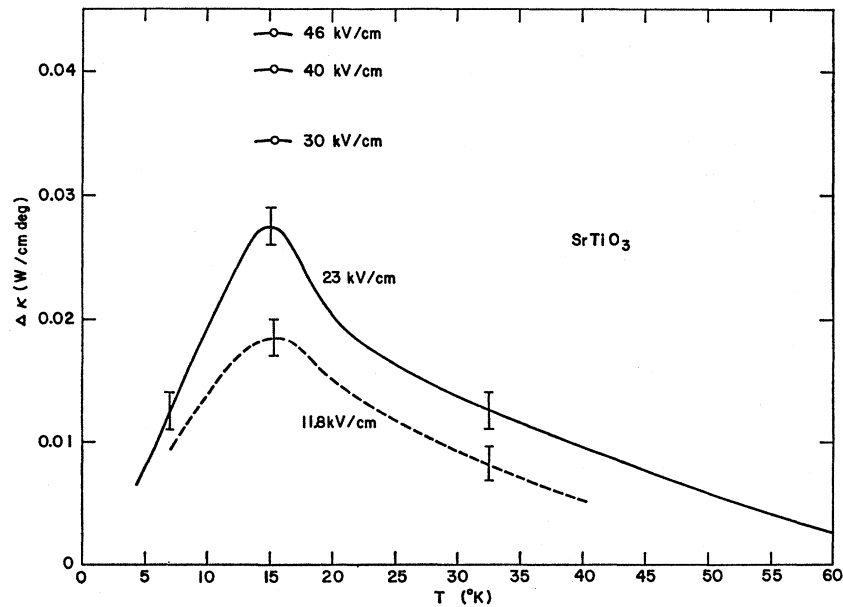


FIG. 2. The change in thermal conductivity $\Delta\kappa = \kappa_E - \kappa$ of SrTiO₃, upon application of an electric field, as a function of the temperature.

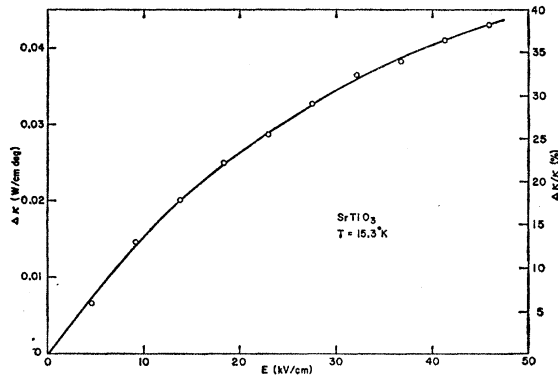


FIG. 3. The change in thermal conductivity $\Delta\kappa = \kappa_E - \kappa$ of SrTiO_3 as a function of the applied electric field.

tion.²¹ Much smaller changes in κ were obtained if this was not the case. Since it is well known^{22,23,14} that a twin-domain structure occurs in all SrTiO_3 crystals below 103°K , it is suggestive to ascribe the above size effect to some kind of preferential crystallographic orientation of these domains, which is energetically preferred in thin crystals, but which can also be enforced in thick crystals by applying an electric field.

KTaO_3

The results obtained for the thermal conductivity of KTaO_3 are shown in Fig. 4 for three different samples. Measurements with applied electric field offer even more difficulties for this material than for SrTiO_3 . Although it was possible to apply to KTaO_3 high enough fields at room temperature, this was in most cases prevented at low temperatures by an electrical breakdown at fields as low as 10 kV/cm. This made it impossible to study the field effect in KTaO_3 in detail. Despite this, it can be seen from Fig. 4 that the field effect is much smaller in KTaO_3 than in SrTiO_3 .

INTERPRETATION

SrTiO_3

Besides the 103°K phase transition, cubic-to-tetragonal nonferroelectric, which has been mentioned already, Lytle²⁴ has claimed additional phase transitions at 65°K , and at 35 to 10°K . All phases were reported to be pseudocubic with ratios of the lattice parameters differing marginally from 1. These additional transformations, which were questioned¹⁴ later on, have found some support from elastic measurements,²⁵ which, however, might be influenced by the domain structure. A fully conclusive confirmation is still missing. Paramagnetic-

²¹ It has been established recently (Refs. 25 and 26) that this transformation occurs at 103°K rather than at 110°K quoted previously.

²² K. A. Müller, *Helv. Phys. Acta* **31**, 173 (1958).

²³ E. Sawaguchi, A. Kikuchi, and Y. Kodera, *J. Phys. Soc. Japan* **18**, 459 (1963).

²⁴ F. W. Lytle, *J. Appl. Phys.* **35**, 2212 (1964).

²⁵ G. Rupprecht and W. H. Winter, *Phys. Rev.* **155**, 1019 (1967).

resonance studies,²⁶ which are very sensitive to symmetry, rather indicate that SrTiO_3 stays in the tetragonal phase between 103°K and helium temperature.

The lattice dynamics of SrTiO_3 has been thoroughly investigated by Cowley,⁸ both experimentally and theoretically. The reported phonon dispersion curves are reproduced in Fig. 5 for reference in connection with the interpretation of our thermal-conductivity results. Cowley has suggested that the 103°K phase transition is due to an accidental degeneracy of TO and LA modes over a considerable region in q space near this temperature. It is believed that this degeneracy is also the cause for some interesting features observed in

TABLE I. Calculation of the field effect in SrTiO_3 .

(1) Relaxation times

(a) Resonance scattering^a:

$$\tau_{\text{res}}^{-1} = c_1 T^2 \omega^2 / \{ [\omega_0^2(T) - \omega^2]^2 + c_2 \omega_0^2(T) \omega^2 \}.$$

(b) Isotope scattering^b:

$$\tau_I^{-1} = (\delta^3 \Gamma / 4\pi v^3) \omega^4 = A \omega^4; \quad v = (k/\hbar) [\Theta \delta / (6\pi^2)^{1/3}],$$

where δ is the cube root of atomic volume, v is the Debye sound velocity, Γ is the disorder parameter, and ω is the angular phonon frequency.

(c) Boundary scattering^c:

$$\tau_B^{-1} = v/LF = B,$$

where L is a typical sample dimension, and F is a geometric factor.

(2) Thermal conductivity^d (for $T < T_{\text{max}}$ and zero electric field)

$$K = GT^3 \int_0^{\Theta/T} \tau_c [x^4 e^x / (e^x - 1)^2] dx, \quad x = \hbar\omega/kT$$

$$\tau_c^{-1} = \tau_{\text{res}}^{-1} + \tau_I^{-1} + \tau_B^{-1}, \quad G = (k/2\pi^2 v) (k/\hbar)^3.$$

(3) Thermal conductivity with electric field

$$\omega_0 \rightarrow \omega_E, \quad \kappa \rightarrow \kappa_E.$$

(4) Parameters used in calculation

$$\begin{aligned} \Gamma &= 3.35 \times 10^{-5}, \\ \Theta &= 700^\circ\text{K}, \\ v &= 5.36 \times 10^5 \text{ cm sec}^{-1}, \\ A &= 2.048 \times 10^{-46} \text{ sec}^3, \\ L &= 10 \mu, \\ B &= 5.36 \times 10^8 \text{ sec}^{-1}, \\ G &= 2.92 \times 10^8 \text{ W deg}^{-4} \text{ cm}^{-1} \text{ sec}^{-1}, \\ \omega_0(T) &: \text{ see Table II.} \end{aligned}$$

(5) Parameters obtained from curve fitting

$$\begin{aligned} c_1 &= 8.707 \times 10^{32} \text{ deg}^{-2} \text{ sec}^{-3}, \\ c_2 &= 3.682, \\ \omega_E/\omega_0 &: \text{ see Figs. 7 and 8.} \end{aligned}$$

^a Used on a heuristical basis. Note that relaxation times of this type were used successfully for interpreting phonon scattering by resonant modes ω_0 in alkali halides; see, e.g., C. T. Walker and R. O. Pohl, *Phys. Rev.* **131**, 1433 (1963).

^b P. G. Klemens, *Proc. Phys. Soc. (London)* **A68**, 1113 (1955).

^c H. B. G. Casimir, *Physica* **5**, 495 (1938).

^d See Ref. 28.

²⁶ K. A. Müller (private communication).

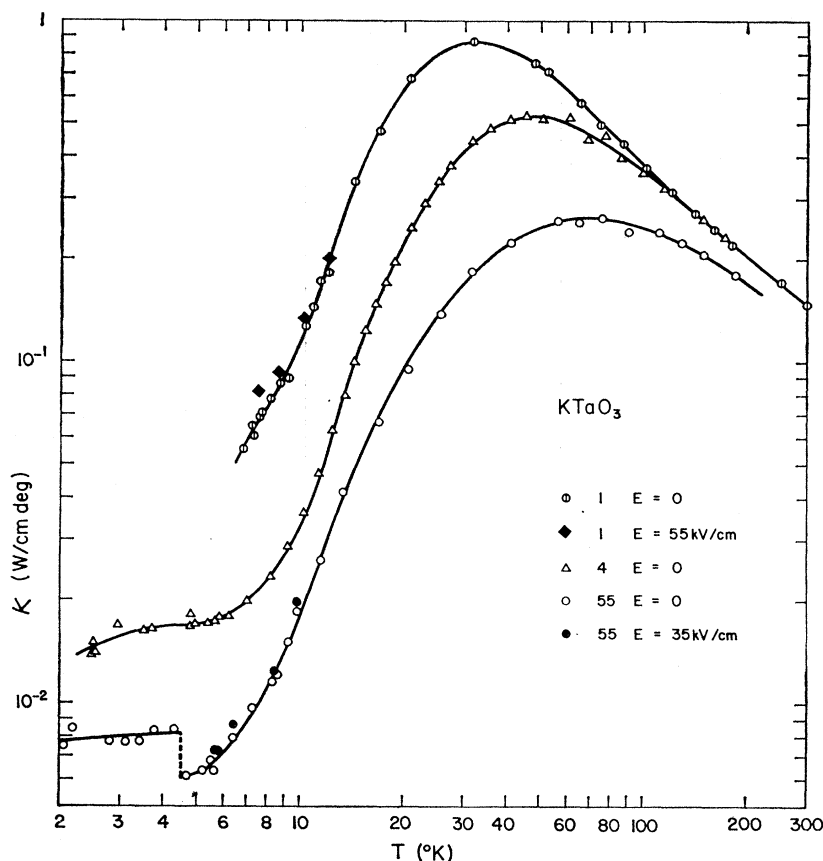


FIG. 4. The thermal conductivity of KTaO_3 as a function of the temperature for zero electric field (\circ , \triangle , \circ) and for an applied electric field (\blacklozenge , \bullet).

the thermal-conductivity curve (Fig. 1). Above the thermal-conductivity maximum a bump is noticed in the curve. Also, the temperature dependence is very weak (about $T^{-0.25}$). In pure insulators and at temperatures below half of the Debye temperature (note that $\Theta \approx 700^\circ\text{K}$ for SrTiO_3),²⁷ the thermal conductivity is known to vary as T^{-1} or stronger; this results from the phonon mean free path which *increases* with decreasing temperature. It is suggested here that a term competing with this behavior arises in materials with strongly temperature-dependent TO modes. If part of the phonon

scattering is due to the interaction of the degenerate or nearly degenerate TO and LA modes, any increase of this degeneracy with decreasing temperature (which occurs according to Fig. 5) then corresponds to a *decrease* in mean free path with decreasing temperature. Obviously, this can lead to a greatly reduced temperature dependence of κ , which is actually observed for SrTiO_3 . The fact that a comparatively low value is obtained for the thermal-conductivity maximum, although the material is of considerable purity and perfectness, also supports the present interpretation. A more quantitative phenomenological description of the results between 20 and 300°K in terms of commonly used relaxation times and the theory of Klemens and Callaway²⁸ was attempted, but thus far has given poor results.

An alternative approach to explain the same feature has been taken by Nettleton.²⁹ He used a model which lumps all temperature-dependent modes into a single mode with angular frequency $\omega_0(q=0)$ proportional to $(T - T_C)^{1/2}$, q being the phonon wave vector and T_C the "Curie" temperature. Taking four-phonon interaction into account, he is able to predict a downward con-

TABLE II. Values used for interpretation.

T ($^\circ\text{K}$)	ω_0^a (sec^{-1})	κ_{exp}^b ($\text{W cm}^{-1} \text{deg}^{-1}$)	$\kappa_B^{(\text{exp})}^b$ ($\text{W cm}^{-1} \text{deg}^{-1}$)
5	1.905×10^{12}	0.54×10^{-2}	1.25×10^{-2}
8	1.955	1.92	3.45
10	2.07	3.65	5.50
14	2.18	8.80	11.50
17	2.29	14.40	17.05
20	2.39	19.50	21.50

^a Obtained by extending curve $\omega_0(T)$ given in Ref. 8 to lower temperatures by scaling with $1/\epsilon(T)$ curve of Ref. 14, according to the Lyddane-Sachs-Teller relation (Ref. 15) $\omega_0^2(T) = \text{const}/\epsilon(T)$.

^b From Fig. 1.

²⁷ Calculated by means of the method of P. M. Marcus and A. J. Kennedy [Phys. Rev. **114**, 459 (1959)] from the elastic constants given by R. O. Bell and G. Rupprecht, Phys. Rev. **129**, 90 (1963).

²⁸ P. G. Klemens, Proc. Roy. Soc. (London) **A208**, 108 (1951); in *Solid State Physics*, edited by F. Seitz and D. Turnbull (Academic Press Inc., New York, 1958), Vol. 7, p. 1; Phys. Rev. **119**, 507 (1960); J. Callaway, *ibid.* **113**, 1046 (1959).

²⁹ R. E. Nettleton, Phys. Rev. **140**, A1453 (1965).

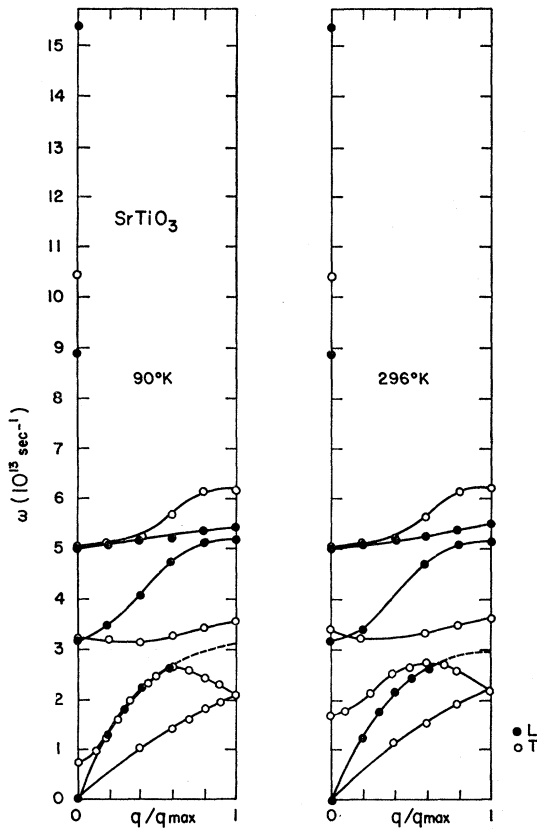


FIG. 5. The phonon spectrum of SrTiO_3 according to Ref. 8: Phonon frequency as a function of the reduced wave vector in the $[100]$ direction, \bullet , longitudinal modes; \circ , transverse modes. The curves are drawn through the experimental points.

vex thermal conductivity curve at about 50°K . In our opinion, however, there is some doubt whether this model (although correct for lower temperatures) is really applicable at temperatures of about 50°K . It seems that the model would also imply an appreciable change in thermal conductivity with electric field as a consequence of the shift in the frequency ω_0 with electric field (see below). However, such an effect is not observed at the temperatures where the bump occurs.

With regard to the results given in Fig. 1, another interesting fact should be pointed out. Below the thermal-conductivity maximum a temperature dependence of $T^{2.7}$ is noticed as opposed to the T^3 law found usually in the boundary-scattering regime. This suggests that boundary scattering is not the limiting process in this temperature range. The same is concluded from the absolute value of κ below 20°K . As mentioned above, a twin-domain structure is observed^{22, 23, 14} in SrTiO_3 below 103°K , with domains of 10 to 30μ width. Taking 10μ as the mean free path, the calculated thermal conductivity due to grain boundary scattering turns out to be higher than what is observed experimentally, suggesting some additional scattering process to be active.

We turn now to the field effect observed for temperatures below 50°K : To understand this effect quantitatively based on the phonon spectrum given in Fig. 5,

one has just to assume that an upward shift is exerted to the TO mode by the applied electric field. This reduces the TO-LA interaction, and thus increases the thermal conductivity. Such a shift is suggested by the strong reduction of the dielectric constant with applied dc field,^{13, 14} and the correlation between dielectric constant and TO frequency.¹⁵ The appearance of the electric-field effect at low temperatures was taken as evidence that an applied electric field shifts the TO mode in the vicinity of $q=0$ only. Based on this, the following model was used for a quantitative interpretation: The modes of the TO branch which are field-dependent are lumped into one mode ω_0 , which is allowed to interact with the other phonons, i.e., the non-field-dependent optic and the acoustical phonons. (This is essentially the same model as used by Nettleton²⁹ to explain the dip observed at high temperatures. However, as mentioned above, such a model seems inapplicable at temperatures above the thermal-conductivity maximum, while it is believed to be pertinent for temperatures below it.) For this process a relaxation time of resonance character has been used on a heuristical basis, the detailed form of which is given in Eq. (1a) of Table I. Other phonon-phonon scattering processes not involving ω_0 are believed to be negligible at these temperatures because of the long mean free path of the pertinent phonons; this includes the field-independent optic modes as well as all acoustic modes, interacting among themselves. In addition to the resonance scattering, we have also included phonon scattering by isotopes and by boundaries for which the expressions are shown, as well, in Table I. The quantities A and B are calculated from the natural abundances of the isotopes and the grain size, and the frequencies ω_0 are obtained as described in Table II. For the zero-field case and for $T \leq 20^\circ\text{K}$ a computer fit of the theoretical expression (Table I) to the experimental curve (Fig. 1) has been carried out, treating the unknown parameters c_1 and c_2 as adjustable. Figure 6 shows that in this manner a close agreement with the experimental data is obtained (dashed curve). The c_1 and c_2 values needed for fitting are given in Table I. For the electric-field case, the frequency ω_0 in the resonance relaxation time τ_{res} is replaced by ω_E , all other parameters being left unchanged. The frequency ω_E is then varied in order to obtain agreement (solid curve in Fig. 6) at any temperature below 20°K with the experimental κ_E values. This determines the shifted frequencies $\omega_E(T)$. A plot of the nonzero-field to zero-field frequency ratio ω_E/ω_0 as a function of temperature is given in Fig. 7. It is seen that an applied electric field of 23 kV/cm causes frequency shifts of more than a factor of 2 (solid curve). Figure 8 shows the corresponding curve (solid line) as a function of the applied field with temperature as a parameter.³⁰ The dashed curves in both figures indicate

³⁰ Note that Figs. 7 and 8 are not completely consistent. This results from the fact that for Fig. 7, $\Delta\kappa$ has been taken with reference to the dashed curve in Fig. 6; while for Fig. 8, $\Delta\kappa$ has been taken with reference to the open circle at 15.3°K in Fig. 6.

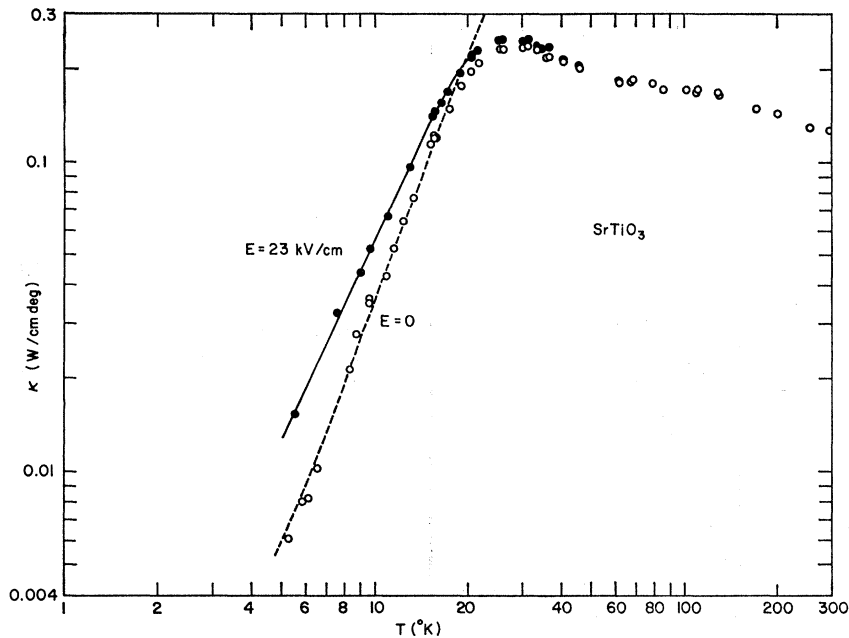


FIG. 6. The thermal conductivity of SrTiO₃ as a function of the temperature without (○) and with (●) an electric field of 23 kV/cm applied to it. The dashed and full curves are theoretical (see text).

the shift one might expect if the Lyddane-Sachs-Teller relation¹⁵ would hold in a rigorous manner for fields different from zero. This seems not to be the case, although it should be pointed out that the model used here is rather crude.

After this work has been completed, Worlock and Fleury¹⁰ determined the TO frequency shift in a more direct manner from a measurement of the Raman effect under an applied electric field.

They report a splitting of the TO mode by the applied field. The two peaks, which are observed, shift unequally with the applied field; while one of them seems to follow almost the Lyddane-Sachs-Teller relation (dashed curve in our Fig. 8), the other peak exhibits a much weaker field dependence (intermediate between dashed and full

curve in our Fig. 8). Thus, considering the crudeness of our model, the results of Worlock and Fleury seem consistent with the conclusions reached in this work.

KTaO₃

In comparing the results in Fig. 4 on KTaO₃ with those on SrTiO₃, the most striking differences are:

- (1) The thermal conductivity exhibits no anomalous behavior above the maximum: No bump is observed in the curve, and the temperature dependence is not nearly as weak as in SrTiO₃; rather, it is in the vicinity of T^{-1} .

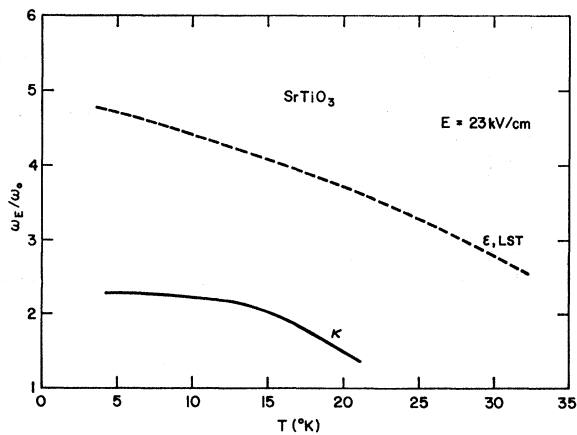


FIG. 7. The ratio of the nonzero-field to the zero-field transverse optical mode frequency as a function of the temperature. Full curve: as determined from the experimental data (Fig. 1) using a simple model (see text); dashed curve: as calculated from the dielectric constant if the Lyddane-Sachs-Teller relation would hold in a rigorous manner for the nonzero-field case.

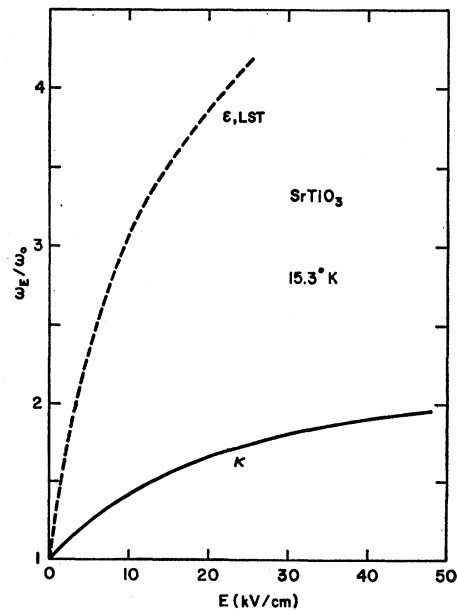


FIG. 8. The ratio of the nonzero-field to the zero-field transverse optical mode frequency as a function of the temperature. Full and dashed curve as described in Fig. 7.

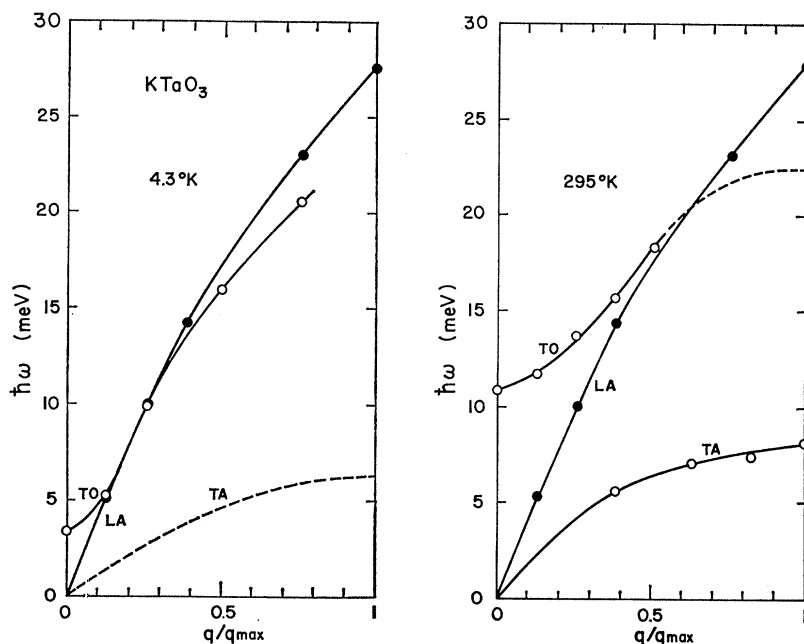


FIG. 9. The phonon spectrum of KTaO_3 according Ref. 11. Phonon energy as a function of the reduced wave vector in the $[100]$ direction. \bullet , longitudinal modes; \circ , transverse modes. The curves are drawn through the experimental points.

(2) The electric-field effect is much smaller in KTaO_3 , a fact which is also confirmed by recent measurements¹⁰ of the Raman effect with applied electric field.

These features can well be understood in terms of the phonon spectrum given in Fig. 9, which was reported recently by Shirane *et al.*¹¹ It was found that the accidental degeneracy of the TO and LA modes (over a considerable region in q space) occurs at a temperature of 4 to 10°K, as compared to 103°K in SrTiO_3 . This means that the TO-LA interaction comes into play at a much lower temperature, so that it cannot affect the thermal conductivity above the maximum, which thus behaves regularly. It also makes clear why the field effect is so much weaker in KTaO_3 , since according to the results in SrTiO_3 it appears that an appreciable field effect might be observable only at a fraction of the degeneracy temperature.

The question was raised¹¹ as to whether the TO-LA mode degeneracy at 4 to 10°K also causes a phase transition, as in SrTiO_3 . Indications pointing in this direction are found indeed in inelastic neutron scattering.¹¹ It is interesting to notice in Fig. 4 that sample 55 shows a discontinuity in the thermal-conductivity curve at 4.5°K which is reproducible. The same effect was observed in a first run on sample 1 at 4.7°K. (On this sample, however, this could not be reproduced later

on, possibly because of breakthrough occurring during the field-effect measurements.) Thus, there is some evidence for a phase transition in KTaO_3 at 4.5°K which will have to be confirmed by crystallographic studies. The transition is felt to be of the nonferroelectric type, since earlier data³¹ as well as some measurements carried out during this work³² reveal no anomaly in the dielectric constant at 4.5°K, in complete analogy to the 103°K transition in SrTiO_3 .

ACKNOWLEDGMENTS

The author is indebted to G. Cullen and J. A. van Raalte for the KTaO_3 crystals, to H. Schoch for valuable technical assistance, and to H. R. Schwarz and W. Kellenberger for programming and computing the curve fitting. Numerous stimulating and enlightening discussions with R. Klein are gratefully acknowledged, and thanks are also extended to E. Fatuzzo and H. Gränicher, as well as to many of the author's colleagues, for helpful conversations, and to P. A. Fleury and K. A. Müller for communicating their results prior to publication.

³¹ S. H. Wemple, Phys. Rev. **137**, A1575 (1965).

³² M. L. A. Robinson and E. F. Steigmeier (private communication).